Multi-Wavelength Analysis of Dwarf Novae Eruptions

K.M.M. McPherson[a,*] and P.J. Meintjes[a]

[a] *Department of Physics, University of the Free State, PO Box 339, Bloemfontein, South Africa*

E-mail: mcphersonkmm@ufs.ac.za, meintjpj@ufs.ac.za

Dwarf novae are a subclass of Cataclysmic variable stars, which are a type of binary system that contain a white dwarf primary star and a main-sequence secondary star (typically a K- or an M-type star) where the secondary star transfers matter onto the white dwarf via Roche-lobe overflow. These binary systems often have an accretion disc. Dwarf novae have outbursts, which are 2-6 magnitude increases in the brightness of the system that usually happen in regular intervals, which aren't necessarily periodic. These outbursts occur on a timescale of the order of days or even years. Occasionally, these sources will go into superoutburst, which are much brighter and last longer than regular outbursts. The standard model that explains this is known as the disc instability model. This involves a thermal-viscous instability that switches the accretion disc between the outburst (hot, ionised) and quiescent (cold, unionised) states. During these processes the non-thermal emission is believed to be driven by magnetic reconnection. The aim of this study is to use the optical light curves of these sources to obtain target of opportunity observations using the MeerKAT telescope when these sources are in outburst. The aim is to see if any radio flux density can be detected from these sources, and to model their spectra using the Van der Laan model, which assumes that the flux density observed in the spectrum is from a superposition of multiple expanding synchrotron emitting blobs.

High Energy Astrophysics in Southern Africa (HEASA2025)
16-20 September, 2025
University of Johannesburg, South Africa

[*] Speaker

PoS(HEASA2025)056

1. Introduction

Cataclysmic variables (CV) are binary systems that contain a white dwarf and a K- or M-type main sequence star where the matter from the K- or M-type is transferred onto the white dwarf via Roche-lobe overflow. This paper is focused on dwarf novae (DNe), a type of CV which has characteristic outbursts of about 2-6 magnitudes in its optical light curve that can last for a few days or even up to 50 days. The frequency of these outbursts varies between each DN, occurring on a daily to yearly time scale in a quasiperiodic manner [1].

The disc instability model is the leading theory that describes these outbursts using the S-curve (shown in figure 1) to visualise the processes that occur. We consider an annulus in the accretion disc. It is important to note that what happens in a single annulus inevitably affects the surrounding annuli and causes a chain reaction that affects the entire disc. If the annulus is in quiescence, the mass flowing into it will exceed the mass flowing out of it. This means that there will be a build-up of material in the annulus, resulting in an increase in surface density, viscosity, and temperature via viscous heating. The annulus now becomes unstable, and the high viscosity of the disc causes an increase in the accretion rate onto the white dwarf. This causes a sudden increase in temperature and an outburst. At this stage, the mass leaving the annulus is greater than the mass entering the annulus, causing a steady decrease in the surface density, temperature, and viscosity. The surface density and viscosity can no longer support the hot ionised disc, which causes it to be unstable. This results in a sharp decrease in temperature through radiative cooling [1].

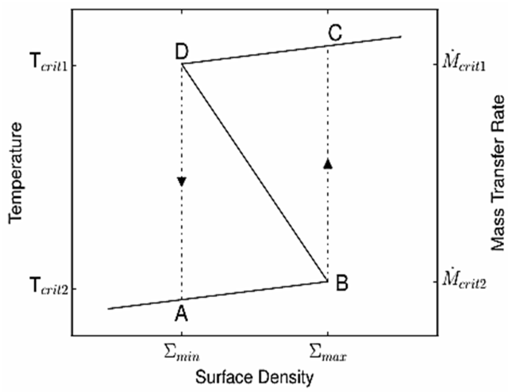

Figure 1: S-curve depicting the disk instability model.Adopted from [1].

The mechanism that is theorised to cause the radio flares in these systems is believed to be the magnetic reconnection process. This occurs when oppositely polarised magnetic fluid zones approach each other and form a "colliding layer" around a null point, and the magnetic and gas pressure force the fluid out of the layer, causing the magnetic field to reconnect. In order for this to occur, we assume that there must be a magnetic field frozen into the disc. When the disc is in the CD branch (outburst), the increased surface density of the disc along with the disc's differential rotation causes a build-up of toroidal as well as vertical (figure 2, left) magnetic fields in the accretion disc, which are now vulnerable to the tearing mode and Parker instabilities, forming vertical magnetic fields that result in a magnetorotational instability and ultimately, magnetic reconnection. A visual representation of this process can be seen in figure 2 (right) [1, 2].

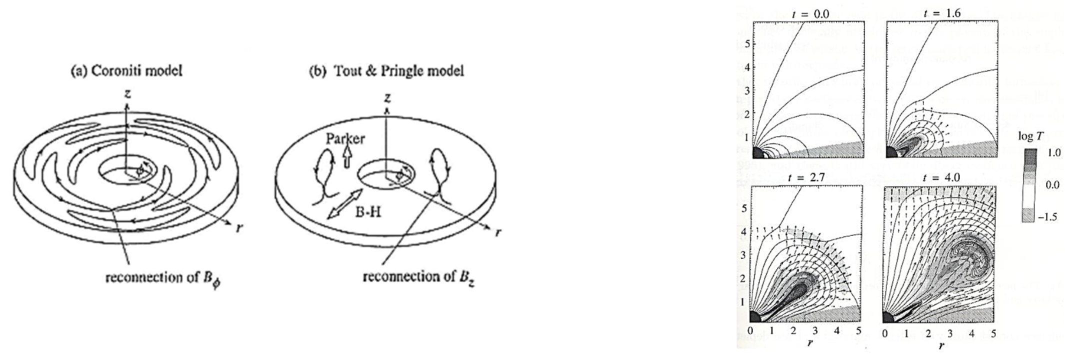

Figure 2: Models of the toroidal (a) and vertical (b) magnetic fields and a visual representation of the magnetic reconnection process. Adopted from [2].

This paper contains an explanation of the various criteria used to obtain suitable sources, as well as the flux density estimates of the sources using the van der Laan model to estimate if the sources will be observable using the MeerKAT radio telescope. The current study follows similar work to that which is presented in [3].

2. The van der Laan Model

The van der Laan model allows us to parametrize the flux density of blobs emitted in the magnetic reconnection process as they expand and radiate through synchrotron radiation [4]. Previous studies show that for the novalike variable AE Aquarii, the flaring activity can be characterised by considering that the spectrum is a result of a superposition of these synchrotron emitting blobs. According to [4, 5], the flux density of a single blob is given by

$$S(\nu,\rho) = S_{m0}\left(\frac{\nu}{\nu_m}\right)^{\frac{5}{2}}\rho^3\frac{1-e^{-\tau_m\left(\frac{\nu}{\nu_m}\right)^{-(\delta+4)/2}\rho^{-(2\delta+3)}}}{1-e^{-\tau_m}} \tag{1}$$

where S_{m0} represents the maximum flux density of the blob at time t_0, ν_m is the frequency at the maximum flux density, τ_m is the optical depth at ν_m, $\rho = (r/r_0)$ represents the ratio of the radius of the blob with respect to its initial radius (r_0), and δ is the electron spectral index. Here, ν_m is given by

$$\nu_m = \nu_{m0}\rho^{-(4\delta+6)/(\delta+4)} \tag{2}$$

where ν_{m0} is the maximum frequency at S_{m0}. Using the fact that the flux density peaks at $\tau_\nu = \tau_m \approx 1$, we can see that

$$\nu_{m0} \approx 2.8\times10^7\left(\frac{E_0}{1MeV}\right)^{\frac{2\delta-2}{\delta+4}}\left(\frac{\delta-1}{\delta+2}N_0 r_{11}\right)^{\frac{2}{\delta+4}} \tag{3}$$

where E_0 is the electron energy, N_0 is the electron number density. The maximum flux density of the blob is given by

$$S_{m0} = A_1 \left[A_2 \frac{\delta - 1}{\delta + 2} \left(\frac{E_0}{1MeV} \right)^{\delta - 1} N_0 r_0^{\frac{4\delta+9}{3}} B_0^{\frac{\delta+3}{6}} \right]^{\frac{3}{2\delta+3}} \nu_m^{\frac{7\delta+3}{4\delta+6}} \tag{4}$$

where B_0 is the magnetic field of the blob and the constants $A_1 = 3.3 \times 10^6 \times 2^{-\delta/2} \pi k / c^2 D^2$ where D is the distance to the source, and $A_2 = (2.8 \times 10^7)^{(\delta+4)/2} / 10^{11}$. By assuming that N_0 cannot be much larger than its equipartition value, we get the following

$$N_0 = A_3 \left[\frac{\delta - 1}{\delta + 2} \left(\frac{E_0}{1MeV} \right)^{-(\delta - 1)} \frac{B_0^{2\delta+9}}{r_0} \right]^{\frac{1}{\delta+5}} \tag{5}$$

where $A_3 = [3.2 \times 10^4 \times 2^{\delta/2} (10^{11})^{1/(\delta+4)}]^{(\delta+4)/(\delta+5)}$. Substituting equations (3), (4), and (5) into equation (1) gives the expected flux densities of individual flare events [4, 5].

3. Source Selection

The process involved using various light curve repositories (CRTS, AAVSO, ASAS-SN) to select a handful of sources that fit specific criteria. The sources had to be within the range of MeerKAT and BOOTES-6, which is a robotic telescope located at the Boyden observatory. The sources must have V-band magnitudes greater than 18 to ensure that they will be easily observable by BOOTES. The sources needed optical light curves that have data for more than one year, ensuring that they are well documented. Lastly, the sources must have frequent outbursts, with multiple outbursts occurring over a one year period. Using these criteria, four sources were identified for this study (seen in table 1).

Source Name	**RA (J2000)**	**Dec (J2000)**	**Quiescent Magnitude**	**Flaring Magnitude**	**Outburst Period**	**Variable Type**
J143145-355205	217.94°	-35.86°	17	15-13	60-70 days	UG[9]
YZ Cancri	122.74°	28.14°	15	13-11	6-16 days[6]	UGSU[9]
X Leonis	147.76°	11.88°	16	13	20 days[7]	UGSS[9]
DT Octantis	280.22°	-83.72°	17	12	30-60 days[8]	UGSU[9]

Table 1: Details of each source. The variable type UG stands for U Geminorum-type variables. UGSU and UGSS stand for SU Ursae Majoris-, and SS Cygni- type variables, which are subclasses of the UG.

The outbursts of most sources were found in literature. Using a Lomb-Scargle periodogram as well as fitting the published periods to their optical light curves, the outburst periods were confirmed. The outburst period of SSS 120424:143145-355205 (J143145-355205) was not found in any literature, therefore Lomb-Scargle analysis was used to roughly estimate the period [13].

4. Results and Discussion

Using the van der Laan model, flux density estimates of the blobs from each source were calculated (shown in figure 3). The calculations were performed by looking at a blob with $\rho = 1$

PoS(HEASA2025)056

(at its initial size) and looking at how the flux density changes as it expands (as ρ increases). The values of ρ have been arbitrarily chosen. The flux density of the blob was estimated using the values found in table 2. A δ value of 2.75 was used for all sources. Looking at the slopes of the peaks of each blob, we can see that the superposition of the blobs gives a spectrum that follows $S_\nu \propto \nu^\alpha$.

Source Name	D (pc)	P_{orb} (days)	$E_{0,a}$ (MeV)	$B_{0,a}$ (G)	$E_{0,b}$ (MeV)	$B_{0,b}$ (G)
J143145-355205	524[14]	0.024	5	500	1	42
YZ Cancri	260[10]	0.087[10]	5	200	1	10
X Leonis	318[15]	0.164[11]	5	300	1	8
DT Octantis	281.7[8]	0.073[12]	5	200	1	13

Table 2: Values used in the models. The orbital periods were used to estimate the average binary separation using the fact that $P^2 \propto a^3$. J143145-355205's orbital period was approximated using Lomb-Scargle analysis [13]. The "a" values for the electron energies and magnetic field represent values that are given under the assumption that the electrons in the blob will have a higher energy caused by the effective acceleration of electrons through magnetic reconnection, with moderate magnetic field values. The "b" values represent magnetic field and electron energies that have been considerably relaxed to show flux densities that are within the range of those previously reported by Deanne Coppejans [17].

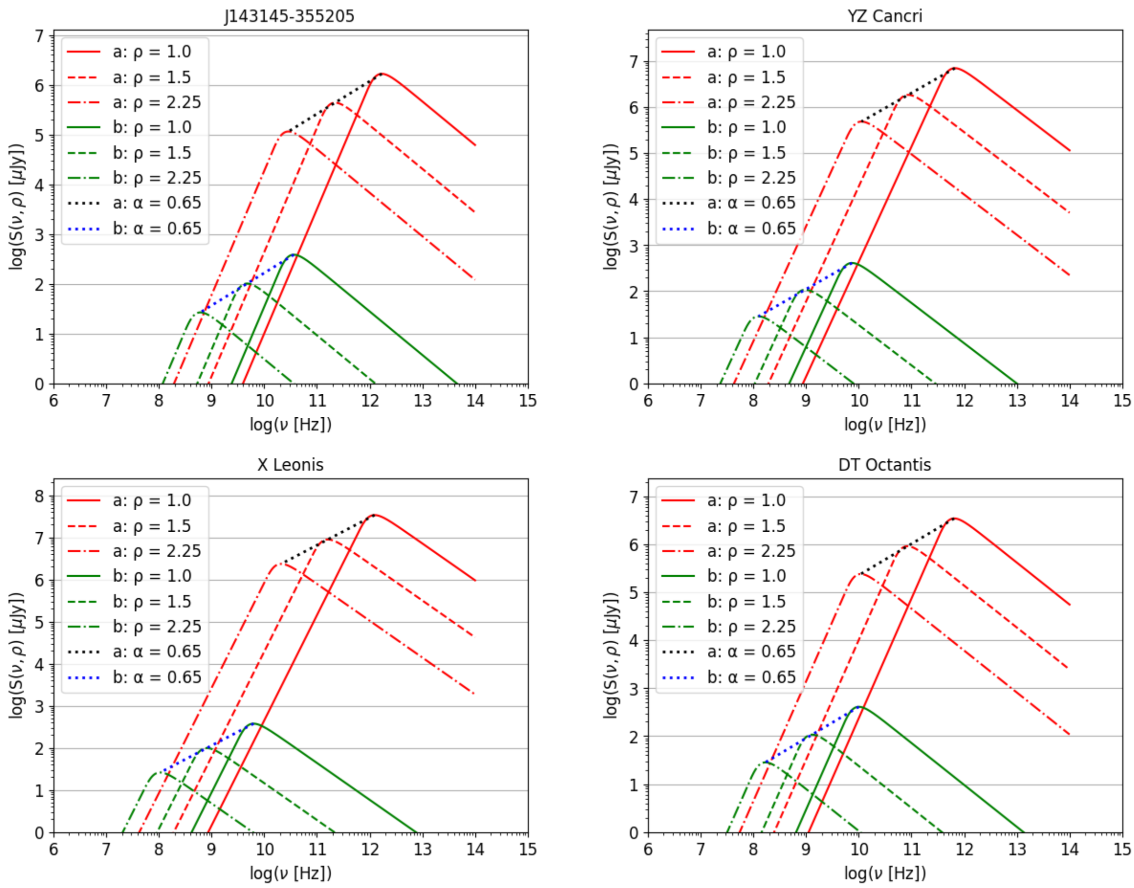

Figure 3: Flux density models of the sources with the case a values in red and the case b values in green.

The flux density estimates have been plotted on one plot for each source with **case a in red** and **case b in green**. We can see from the flux density values, based on preliminary and perhaps optimistic estimates for the a-values of E_0 and B_0, that the sources should readily be detectable by the MeerKAT array in the L-band, which has a flux density limit threshold of about 10 μJy [16]. The modelled flux densities obtained using the a-values are well above this range (peak flux densities about 10000 times larger); however, the values used in the model are within reason. The b-values of E_0 and B_0 have been considerably relaxed in order to see which values give peak flux density values which are above the MeerKAT threshold, with the estimated peak flux density values being between about 30-700 μJy. The flux density estimates show that considerably weaker electron energies and magnetic field strengths may also allow for observable flux density values. The sources investigated in a survey by Deanne Coppejans showed peak flux densities of about 15-60 μJy [17], which are within the ranges of the flux density estimates obtained with the b-values. With actual flux density data, it may be possible to further constrain the values of B_0, E_0, and δ for each blob in each source.

5. Conclusion

The models show that, within a reasonable range, the estimated parameters for each of the sources allow for reasonable flux density levels that will be observable within the MeerKAT limit. This is shown for sources with considerably relaxed magnetic field strengths and electron energies, as well as for sources with weaker magnetic field strengths that have higher electron energies caused by the effective acceleration of electrons through magnetic reconnection. From the graphs, the observed peak flux density will be from fresher blobs, which is expected. Using the optical light curves of these sources, one can establish possible epochs for when the sources flare. This opens the door for target of opportunity observations with the MeerKat telescope to observe possible radio flares.

6. Acknowledgements

The authors thank the organisers for the publication invitation, as well as the University of the Free State research development directorate for their financial support, which is enabling the author to pursue his Master's studies. The authors extend their gratitude to the University of Johannesburg for hosting the conference. The authors thank the referee for very useful and constructive comments.

References

[1] D. Coppejans, *Multi-wavelength Accretion Studies of Cataclysmic Variable Stars*, Radboud University Nijmegen (2016), https://docslib.org/doc/3911552/multi-wavelength-accretion-studies-of-cataclysmic-variable-stars

[2] P.J. Meintjes, *Magnetic Reconnection and Transient Phenomena in Accretion Driven Systems*, in proceedings of *HEASA2016*, Proceedings of Science, 2016, DOI: https://doi.org/10.22323/1.275.0032

[3] J. Kersten et al. *A MeerKAT survey of nearby dwarf novae: I. New detections*, *MNRAS* **539** (2025) 1894-1907

[4] P.J. Meintjes & L.A. Venter, *Modelling the continuous radio outbursts in AE Aquarii*, *MNRAS* **341** (2003) 891–900

[5] T.S. Bastian et al. *Radio Flares from AE Aquarii: A Low-power Analog to Cygnus X-3?*, *The Astrophysical Journal* **324** (1988) 431-440

[6] J. van Paradijs et al. *A 60-night campaign on dwarf novae – I. Photometric variability of SU UMa and YZ Cnc*, *MNRAS* **267** (1994) 465-472

[7] P. Szkody et al. *Outburst Spectra of 11 Dwarf Novae*, *ApJS* **73** (1990) 441

[8] V. Simon & H. Edelmann, *Long-Term Activity of a Little Known Dwarf Nova DT Octantis* *Astrophysical Bulletin* **74** (2019) 490-496

[9] T. Jayasinghe et al. *The ASAS-SN catalogue of variable stars – II. Uniform classification of 412 000 known variables*, *MNRAS* **486** (2019) 1907-1943

[10] D. Coppejans et al. *Dwarf nova-type cataclysmic variable stars are significant radio emitters*, *MNRAS* **463** (2016) 2229-2241

[11] A.W. Shafter & R.P. Harkness, *Spectroscopic orbits for the dwarf novae X Leonis and SS Aurigae*, *The Astrophysical Journal* **92** (1986) 658-663

[12] T. Kato et al. *Survey of period Variations of Superhumps in SU UMa-Type Dwarf Novae. VII: The Seventh Year (2014-2015)*, *Publications of the Astronomical Society of Japan* **67** (2015) 1-116

[13] J.T. VanderPlas, *Understanding the Lomb-Scargle Periodogram*, *ApJS* **236** (2018) 16

[14] A.S. Oliveira et al. *Exploratory Spectroscopy of Magnetic Cataclysmic Variables Candidates and Other Variable Objects. II*, *The Astronomical Journal* **159** (2020) 114

[15] T. Ak et al. *A new absolute magnitude calibration with 2MASS for cataclysmic variables*, *New Astronomy* **12** (2007) 446-453

[16] J.D. Wagenveld et al. *The MeerKAT Absorption Line Survey Data Release 2: Wideband continuum catalogues and a measurement of the cosmic radio dipole*, *A&A* **690** (2024) A163

[17] R. Fender & P. Woudt, *ThunderKAT: The MeerKAT Large Survey Project for Image-Plane Radio Transients*, in proceedings of *MeerKAT Science: On the Pathway to the SKA*, Proceedings of Science, 2016, DOI: https://doi.org/10.22323/1.277.0013